

# Excited hadrons on the lattice

## State of the art and future challenges

Christof Gatttringer <sup>a</sup>

Universität Graz, Institut für Physik, FB Theoretische Physik, 8010 Graz, Austria

Received: date / Revised version: date

**Abstract.** We review the techniques of lattice QCD calculations for excited hadrons with light quarks and outline the future challenges that are faced in calculations with fully dynamical fermions.

**PACS.** 11.15.Ha Lattice QCD

## 1 Introduction

In the last 20 years the lattice approach has evolved into a powerful quantitative tool for obtaining non-perturbative results from ab-initio QCD calculations. A revolutionary breakthrough was the understanding of chiral symmetry on the lattice, which may be implemented by using a lattice Dirac operator that obeys the Ginsparg-Wilson equation [1]. Thus lattice QCD is now conceptually ready for calculations with fully dynamical light quarks, and as algorithms and computer technology are evolving rapidly, more challenging problems are considered.

An prominent example for this type of more advanced calculations is the analysis of excitations of hadrons. Excited states are much harder since they, as we will outline in the next section, appear only in sub-leading terms of the Euclidean correlators one analyzes on the lattice. Although powerful methods are available for tackling this problem, it is still a challenge to construct hadron interpolators that have a strong overlap with the excitations, and at the same time may be implemented numerically in a cost-efficient way.

About 5 years ago several groups started to systematically explore hadronic excitations using lattice QCD [2]. A strong motivation for this enterprise is, e.g., the unresolved nature of the first positive parity excitation of the nucleon, the N(1440) Roper state. Although calculations at relatively large volumes with light quarks were performed, there is still no definitive answer to the Roper puzzle from the lattice. In particular the role of dynamical sea quarks still has to be understood more clearly. Nevertheless, the Roper problem has considerably pushed the development of the techniques for excited hadrons.

After a brief introduction to lattice methods, in this contribution we review the recent developments and outline how a state of the art calculation for excited hadrons

with light quarks proceeds. We illustrate the current status by discussing a few selected results in more detail.

The above mentioned progress towards fully dynamical simulations with light quarks gives rise to new challenges: So far most of the calculations were done in the quenched approximation where excited states cannot decay. The same is true for a dynamical calculation when the quarks are heavy such that decays are not possible due to kinematical reasons. However, slowly data from simulations with light dynamical quarks become available and the problem of particle decay and scattering states has to be faced. In the continuum a scattering state has a continuous spectrum of energies and for a particular value of the relative momentum its energy may be degenerate with the energy of a bound state. In the Euclidean correlator one studies on the lattice, this degeneracy leads to a mixing of scattering and bound states. The tools for disentangling the two types of states are ready in principle - one uses a finite volume analysis - but the implementation of these ideas in full lattice QCD calculations is still in its infancy. We briefly address these problems, together with other future challenges, such as the evaluation of matrix elements for excited states.

## 2 Excited states in lattice QCD

### 2.1 Euclidean correlators on the lattice

Before we come to discussing excited states on the lattice, we need to review the central tool in lattice QCD, Euclidean correlators. In any lattice calculation one evaluates numerically the correlators of some operators  $\hat{O}$ . The Euclidean correlator of two operators  $\hat{O}_1, \hat{O}_2$  is defined as

$$\langle O_2(t) O_1^\dagger(0) \rangle = \lim_{T \rightarrow \infty} \frac{1}{Z_T} \text{Tr} [\hat{O}_2 e^{-t\hat{H}} \hat{O}_1^\dagger e^{-(T-t)\hat{H}}], \quad (1)$$

$$Z_T = \text{Tr}[e^{-T\hat{H}}]. \quad (2)$$

<sup>a</sup> Invited plenary talk at NSTAR 2007, September 5-8 2007, Bonn, Germany

In this expression  $\hat{H}$  is the QCD Hamiltonian and  $t$  and  $T$  are real numbers, often referred to as Euclidean time.

The interpretation of the Euclidean correlators is obtained with the help of the (unknown) eigenstates  $|n\rangle$  of the Hamiltonian which obey  $\hat{H}|n\rangle = E_n|n\rangle$ , where  $E_n$  denotes the energy of the eigenstate  $|n\rangle$ . If one uses them to compute the traces in (1) and (2), and inserts the unit in the form  $\mathbb{1} = \sum_n |n\rangle\langle n|$  to the left of  $\hat{O}_1$  in (1), one finds

$$\langle O_2(t) O_1^\dagger(0) \rangle = \sum_n \langle 0 | \hat{O}_2 | n \rangle \langle n | \hat{O}_1^\dagger | 0 \rangle e^{-tE_n}. \quad (3)$$

In this spectral representation for the Euclidean 2-point function, the sum runs over all eigenstates  $|n\rangle$  of the QCD Hamiltonian. Each term comes with a Boltzmann factor containing the corresponding energy  $E_n$ . The energies are normalized relative to the vacuum state  $|0\rangle$  with energy  $E_0 = 0$ . The Boltzmann factors are multiplied with matrix elements of the operators  $\hat{O}_i$  between the vacuum state  $|0\rangle$  and a physical state  $|n\rangle$ .

The spectral representation (3) is a powerful tool. If one, e.g., wants to compute the mass of the nucleon, one uses for both  $\hat{O}_1$  and  $\hat{O}_2$  an operator  $\hat{O}_N$  with the quantum numbers of the nucleon. For this choice the matrix element  $\langle n | \hat{O}_N^\dagger | 0 \rangle$  is non-vanishing only for those terms in the sum, where  $|n\rangle$  is the state  $|N\rangle$  of the nucleon or one of its excitations  $|N'\rangle, |N''\rangle \dots$ . Thus we obtain:

$$\langle O_N(t) O_N^\dagger(0) \rangle = \langle 0 | \hat{O}_N | N \rangle \langle N | \hat{O}_N^\dagger | 0 \rangle e^{-tE_N} + \dots \quad (4)$$

Obviously we can extract the energy of the nucleon from the exponential decay of the Euclidean correlator. Furthermore, the overall factor is related to the matrix element of our operator with the physical nucleon state  $|N\rangle$ .

Having convinced ourselves, that the Euclidean correlator can be used to extract energies and physical matrix elements, we need to discuss the way the Euclidean correlators are evaluated in lattice QCD. Instead of the unknown eigenstates of the QCD Hamiltonian, one uses eigenstates of the field operators for computing the trace in (1). The exponential function of the Hamiltonian is treated with the help of the Trotter formula, which introduces an auxiliary direction that in the end gives rise to a 4-dimensional lattice formulation for the Euclidean correlation function, given by

$$\langle O_2(t) O_1^\dagger(0) \rangle = \quad (5)$$

$$= \frac{1}{Z} \int \mathcal{D}[G, \bar{q}, q] e^{-S[G, \bar{q}, q]} O_2[G, \bar{q}, q]_t O_1^\dagger[G, \bar{q}, q]_0,$$

$$Z = \int \mathcal{D}[G, \bar{q}, q] e^{-S[G, \bar{q}, q]}. \quad (6)$$

The Euclidean correlation function is represented as a path integral over all degrees of freedom, the gluons  $G$  and the quark fields  $\bar{q}, q$ . All fields live on a 4-dimensional lattice, and the path integration  $\mathcal{D}[G, \bar{q}, q]$  is implemented as the product of the integrals over the classical degrees of freedom on all lattice points. Each configuration of the fields  $G, \bar{q}, q$  is weighted with the Boltzmann factor

$\exp(-S)$ , where  $S[G, \bar{q}, q]$  is a lattice discretization of the QCD action (derivatives are replaced by finite differences on the lattice etc). In the path integral the operators  $\hat{O}_i$  appear as monomials  $O_i$  of the classical field variables  $G, \bar{q}, q$ . We will refer to these monomials as *interpolators* from now on. The Euclidean time arguments  $t$  and  $(t=)0$  determine from which time-slice of the 4-dimensional lattice the field variables are taken for building the interpolators.

The expression (5) has the form of an expectation value for a statistical system in the canonical ensemble. Thus the numerical methods from statistical mechanics, in particular Monte Carlo simulation techniques, can be taken over to lattice QCD. Using these we can evaluate the Euclidean correlators numerically and extract the results for energies and matrix elements using the spectral representation (3). However, we stress at this point, that the Monte-Carlo methods which are used for evaluating the Euclidean correlators give rise to statistical errors. As we will see below, this limited accuracy implies that special methods for extracting the physical observables from the correlators have to be developed.

## 2.2 Why are excited states so difficult?

Having outlined the basic steps of a lattice calculation, we can return to the problem of excited states. We have discussed that by selecting suitable interpolators with the quantum numbers  $I, J, P, C$  we can project onto the states we want to analyze, and the example of Eq. (4) illustrates how to study the positive parity nucleon channel. However, when we want to consider the first positive parity excitation of the nucleon, the N(1440) Roper state, we find that this state has the same quantum numbers  $\frac{1}{2}^+$  as the nucleon ground state. Thus all we can obtain from our Euclidean correlator  $\langle O_N(t) O_N^\dagger(0) \rangle$  is a sum of exponentials

$$\langle O_N(t) O_N^\dagger(0) \rangle = \langle 0 | \hat{O}_N | N \rangle \langle N | \hat{O}_N^\dagger | 0 \rangle e^{-tM_N} + \langle 0 | \hat{O}_N | N' \rangle \langle N' | \hat{O}_N^\dagger | 0 \rangle e^{-tM_{N'}} \dots, \quad (7)$$

where  $|N'\rangle$  denotes the first excited state (with positive parity) and  $M_{N'}$  is the corresponding mass (from now on we use interpolators projected to vanishing momentum, such that the energy reduces to the mass,  $E_i = M_i$ ). The dots indicate the contributions of higher excitations with positive parity, such as the N(1710). We stress that negative parity states, e.g., N(1535) and N(1650), do not contribute in the tower of excitations, since the parity of our lattice interpolator  $O_N$  was chosen positive.

Eq. (7) illustrates clearly why excitations are much harder to extract: The spectral decomposition of the Euclidean 2-point function is dominated by the exponential decay from the lightest mass  $M_N$ . Only the sub-leading term contains the mass  $M_{N'}$  of the first excitation we want to study and this contribution is suppressed exponentially for increasing  $t$  with a factor of  $\exp(-(M_{N'} - M_N)t)$ . This implies that only for small values of  $t$  we can hope to see

a signal of the first excitation. For higher excitations the situation is even worse.

Although the signals of the excited states are suppressed exponentially, several different techniques for extracting their spectrum have been applied to the Euclidean correlators. In the next section we will discuss in detail the variational method [10,11]. However, also other approaches have been tried [12]. These attempts employ advanced fitting techniques or other analysis tools for getting both the leading and the sub-leading exponential or even try to reconstruct the spectral density of the two point function. The results typically suffer from the statistical errors which make multi-exponential fits rather unstable and from the fact that excitations produce significant contributions only for small  $t$ . Consequently only a limited amount of information is available. In general the impression is that the alternative methods [12] have not reached the quality of results from the variational method which we discuss in detail in the next section.

### 3 Lattice technology for excited states

#### 3.1 The variational method

In the last section we have addressed the problem of extracting excited state masses from the sub-leading exponentials of Euclidean correlators. The decisive advantage of the variational method [10,11] is, that it extracts more information from the system by analyzing more than a single correlator. Again we use our example of the nucleon to illustrate this point. It is easy to check that the following two interpolators have the quantum numbers of the nucleon ( $C$  denotes the charge conjugation matrix),

$$O_{N_1}(x) = \epsilon_{abc} [u_a^T(x) C \gamma_5 d_b(x)] u_c(x), \quad (8)$$

$$O_{N_2}(x) = \epsilon_{abc} [u_a^T(x) C d_b(x)] \gamma_5 u_c(x). \quad (9)$$

Consequently both of them should give rise to Euclidean correlators that can be used to compute properties of the nucleon and of its excitations.

We illustrate the effect of using different interpolators in Fig. 1 (taken from [8]), where we compare Euclidean correlators for different interpolators with the quantum numbers of the pion. The correlators are plotted as a function of the Euclidean time  $t$ , normalized such that they are 1 at  $t = 1$ . Since we use a logarithmic scale on the vertical axis, the exponential factor  $\exp(-tM)$  gives rise to straight lines with slope  $-M$ . It is obvious, that beyond  $t = 5$  the different correlators all show the same slope which corresponds to the mass  $M$  of the ground state. However, for small  $t$  the correlators have a different admixture of exponential terms  $\exp(-tM')$ , where  $M' > M$  is the mass of an excitation with the same quantum numbers. If an interpolator couples strongly to such an excitation, this produces a steeper slope at small  $t$ .

The central idea of the variational method is to use not only a single one of the possible correlators, but a whole  $r \times r$  matrix of correlators,

$$C_{ij}(t) = \langle O_i(t) O_j(0)^\dagger \rangle, \quad i, j = 1, 2 \dots r, \quad (10)$$

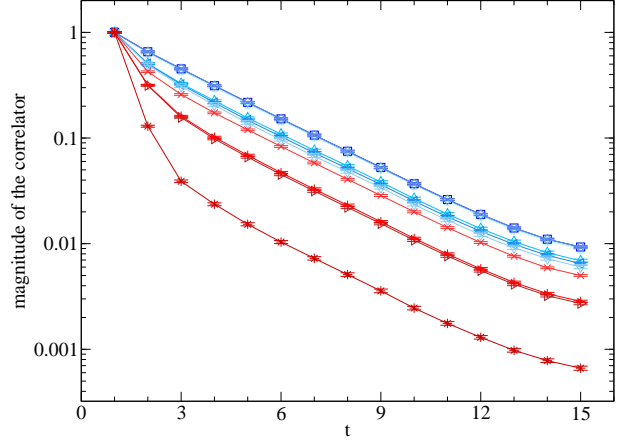


**Fig. 1.** Euclidean correlators for different interpolators with the quantum numbers of the pion. We plot the correlators as a function of Euclidean time  $t$ , using a logarithmic scale for the vertical axis.

where each of the interpolators  $O_i$ ,  $i = 1, 2, \dots, r$  has the quantum numbers of the channel one is interested in. It is obvious, that such a correlation matrix extracts more information from the system than a single correlator.

The determination of the physical observables from the correlation matrix can be cast into an elegant form [11]. One considers the generalized eigenvalue problem

$$C(t) \mathbf{v}^{(n)} = \lambda(t)^{(n)} C(t_0) \mathbf{v}^{(n)}, \quad (11)$$

where  $t_0 < t$  is a timeslice used for normalization. Exploring the particular form of the spectral representation of the correlation matrix (compare Eq. (3)),

$$C_{ij}(t) = \sum_n \langle 0 | \hat{O}_i | n \rangle \langle n | \hat{O}_j^\dagger | 0 \rangle e^{-t M_n}, \quad (12)$$

one can show, that the ordered eigenvalues  $\lambda^{(1)} > \lambda^{(2)} > \lambda^{(3)} > \dots$  behave as

$$\lambda^{(n)}(t) = e^{-(t-t_0)M_n} [1 + \mathcal{O}(e^{-(t-t_0)\Delta_n})], \quad (13)$$

where  $M_n$  is the mass of the  $n$ -th state and  $\Delta_n$  the distance of  $M_n$  to the neighboring mass. Thus the ground- and excited states are disentangled, and each mass appears in an individual eigenvalue. The largest eigenvalue corresponds to the ground state mass  $M_1$ , the second largest eigenvalue to the mass  $M_2$  of the first excitation et cetera.

The fact that in Eq. (13) the ground- and excited states are separated into individual channels allows for simple two-parameter fits of the eigenvalues. The corresponding ground- and excited state masses can be extracted in a stable and transparent way.

We illustrate the power of the variational method in Fig. 2, where we plot the eigenvalues of the correlation matrix, again showing the example of the pion already used in Fig. 1. The figure clearly demonstrates that, when plotted on a logarithmic scale, the slopes for the eigenvalues are different, corresponding to the different masses of the ground- and excited states.

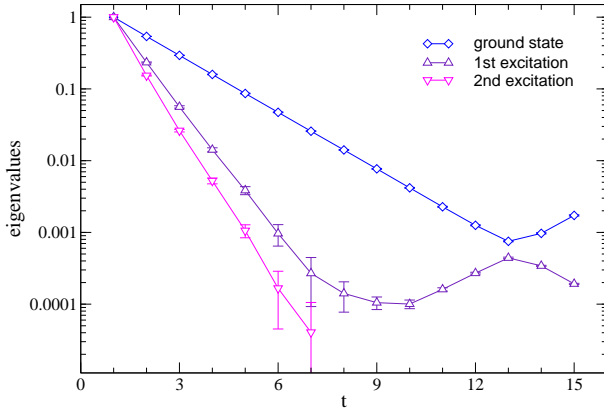


**Fig. 2.** Eigenvalues of the correlation matrix as a function of the Euclidean time. The data are again for the example of the pion, already used in Fig. 1.

### 3.2 Constructing a basis of interpolators

As any variational method, also the application to the excited states problem can only be as good as the basis of interpolators  $O_i$  one uses. Good interpolators should have several properties: 1) They should generate states from the vacuum that are as orthogonal to each other as possible; 2) These states should have a large overlap with the physical states; 3) The construction of the interpolators should be such that they can be implemented numerically in a cost-efficient way.

Several remarks are in order here: The true structure of the wave function of a physical state is unknown. Thus for constructing interpolators with a “large overlap” with the true physical wave function, only an educated guess, e.g., based on models is possible. However, even with a poor guess the method gives rise to the correct result, but the quality of the data might be poor. In practice, typically a large set of interpolators is implemented and subsequently the set of interpolators is reduced such that only the combination with the best signal to noise ratio is kept. If, e.g., an interpolator couples only very weakly to physical states, it will mainly contribute noise to the data, and should be left out in the analysis. An important consistency check of the method is to compare the results from different choices of the interpolators and to ensure that they agree within error bars.

What are the different building blocks we can use for constructing hadron interpolators? The example of the nucleon, given in Eqs. (8), (9), illustrates that different Dirac structures may be used to obtain different interpolators with the same quantum numbers. This freedom typically gives rise to two or three (depending on the channel) different hadron interpolators with the same quantum numbers  $I, J, P$  and  $C$  (where applicable). The different Dirac structures are an important ingredient, but obviously not enough for analyzing the tower of all excitations. It is generally believed, that for a proper description of excited hadrons non-trivial spatial wave functions are essential.

Recently the lattice community started to systematically explore the possibility of implementing non-trivial spatial wave functions [3]–[8] in hadron interpolators. Two different approaches for constructing such wavefunctions on the lattice are used:

Basak *et al* have constructed large sets of possible hadron interpolators by using quark fields on lattice sites displaced relative to each other, typically involving nearest or next-to-nearest neighbors [7]. The operators were classified with respect to irreducible representations of the symmetry group of the hyper-cubic lattice, and in this way the quantum numbers were assigned.

A different strategy was followed in the work of the Graz-Regensburg group [3]–[6], [8]. This approach is based on so-called Jacobi smeared quark sources [9], which is essentially a gauge covariant diffusion process, that leads to an s-wave type of wave function for an individual quark. Combining Jacobi-smeared sources of different width allows for radial wave functions with nodes. Application of an additional covariant derivative gives rise to p-wave type wave functions [8].

It is important to understand that the different interpolators one uses in the variational approach are just the basis one offers to the system. The relative weights of the basis elements are not prescribed, but come out of the variational calculation. Once the generalized eigenvalue problem (11) is solved and the eigenvectors  $v^{(n)}$ ,  $n = 1, 2 \dots r$  are known, one can define new interpolators  $\tilde{O}^{(n)}$  as linear combinations of the original interpolators  $O_i$ ,

$$\tilde{O}^{(n)} = \sum_{i=1}^r v_i^{(n)*} O_i, \quad (14)$$

with the complex conjugate (denoted by  $*$ ) entries  $v_i^{(n)*}$  of the  $n$ -th vector as coefficients. The new interpolators  $\tilde{O}^{(n)}$  are optimal within the given basis of interpolators  $O_i$  in the sense that they give rise to orthogonal correlation functions,

$$\langle \tilde{O}^{(m)}(t) \tilde{O}^{(n)\dagger}(0) \rangle = \lambda^n(t) \delta_{n,m}, \quad (15)$$

as can be shown in a few lines of algebra. Thus the variational method determines through the eigenvectors which linear combinations of the basis interpolators best describe a physical state. In principle the eigenvectors can be functions of the Euclidean time  $t$ . It was observed, that the eigenvectors are essentially independent of  $t$  in the range where the eigenvalues are dominated by a single exponential. In Fig. 3 we illustrate this behavior for the eigenvector corresponding to the ground state, again using the pion example. Comparison with Fig. 2, where the corresponding eigenvalues are plotted, shows that indeed the ground state eigenvalue falls on a straight line up to  $t = 12$ , exactly the range where the eigenvector shown in Fig. 3 displays plateaus for its entries. The property that also the eigenvectors show a signal stable in  $t$  is an important technical tool for identifying the different states and for the determination of fit ranges.

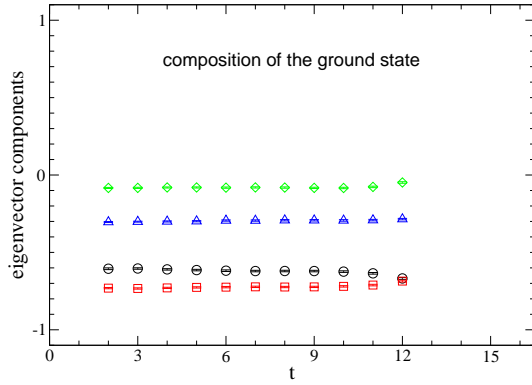


**Fig. 3.** Entries of the first eigenvector of the generalized eigenvalue problem for the pion example already used in Figs. 1,2. The entries are plotted as a function of the Euclidean time  $t$ .

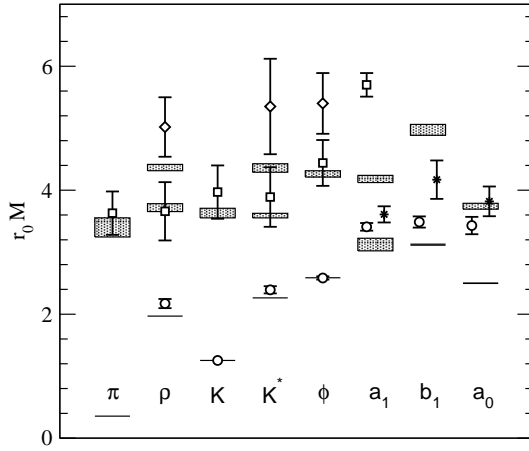


**Fig. 4.** Final results for excited mesons taken from [5]. The horizontal bars are the experimental data, the symbols correspond to the lattice results. All masses are given in units of the Sommer scale  $r_0 = 0.5 fm$ .

## 4 Results and future challenges

### 4.1 Some selected results

Having outlined the ingredients of an excited state calculation in lattice QCD, let us now present some selected results. We begin with discussing the outcome of a quenched calculation for excited mesons [5]. The calculation is based on meson interpolators constructed with the Jacobi smearing techniques outlined in the last section. The quark propagators were computed for several different values of the light quark masses and the results for the meson spectra were extrapolated to the chiral limit. The scale was set with the Sommer parameter and the value of the strange quark mass was determined from the  $K^+$  meson.

In Fig. 4 we show the results for the mass spectrum in different meson channels. The bars are the experimental numbers and the symbols are the lattice results. The errors for the lattice data are statistical errors. The plot shows that for pseudoscalar and vector mesons the lattice results

agree well with the experimental values. The ground state masses typically are correct within 5 percent (10% for the  $\rho$ -meson) and one or two excited states can be calculated which for the first excitations agree with the experimental values within error bars. For the axialvector/tensor mesons the results are less convincing and we believe that here the set of basis interpolators is still not rich enough. Finally for the scalar channel the lattice data seem to coincide with the experimental mass of the first excitation. Understanding the true nature of the scalar meson ground state is an interesting story of its own – it could, e.g., be a tetraquark state – and for a snapshot of the ongoing lattice work on this problem we refer the reader to the recent review [13].

Let us now come to discussing some results for baryons [6]. This quenched calculation is again based on the variational method with basis interpolators constructed with Jacobi smearing. As for the meson case, the light quark masses were extrapolated to the chiral limit and the strange quark mass was set using the  $K^+$  as input.

Fig. 5 shows the results for positive parity in the lhs. plot, while the rhs. is for negative parity. For both parities the ground state masses come out reasonably well – typically with less than 5 percent deviation from the experimental numbers. As for the meson case one is wondering at this point why the quenched approximation is working so well. An exception is the positive parity  $\Delta^{++}$  ground state which typically comes out about 20% too high [2]. A completely different story are the excited positive parity states. They come out typically 25% too high. Several possible reasons for this failure to describe these Roper-like states have been put forward, such as the quenched approximation, too small spatial lattice volumes and the fact that the light quark masses used still might be too large to capture the chiral dynamics necessary to get the masses right [2]. In general the opinion is, that the Roper puzzle will be solved only when dynamical simulations with light quarks on large volumes are completed. This is certainly an expensive enterprise, but the whole lattice community is pushing in this direction, and once these data are available, they will certainly be used for studying excited hadrons.

To conclude the discussion of the baryons with a more positive aspect, we stress that the negative parity states come out very nicely. The lattice typically produces results that are on top of the experimental numbers. For a better resolution of the splitting between the ground- and the first excited state the error bars will have to be reduced. Nevertheless the results are sufficiently reliable, such that the lattice can make a prediction for states in the  $\Xi$  and  $\Omega^{--}$  channels, where the corresponding masses are not yet well established experimentally (filled symbols in Fig. 5).

### 4.2 Upcoming challenges

Let us finally come to the challenges that are waiting for excited state calculations on the lattice in the near future. We have already stressed the point that the quenched approximation is the big unknown in the current results for



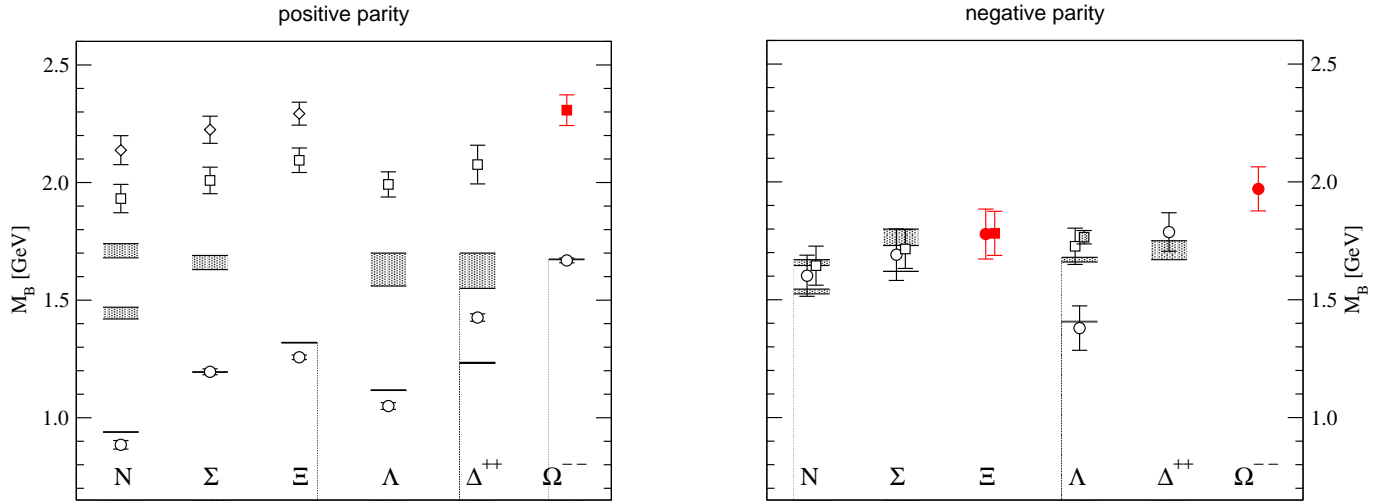


**Fig. 5.** Final results for excited baryons taken from [6]. The horizontal bars are the experimental data, the symbols correspond to the lattice results. In the lhs. plot we show the results for positive parity baryons, while the rhs. is for negative parity.

excited hadrons. We have also addressed the problem with the mixing to scattering states which has to be faced when light dynamical fermions are considered. In principle the techniques for disentangling scattering and bound states are ready to go [14]: For scattering states the relative momentum is quantized in multiples of the Matsubara frequency  $2\pi/L$ , where  $L$  is the spatial extent of the lattice. Thus the energies of scattering states show a power-like dependence on  $1/L$  which is absent for bound states, and comparing the results on different volumes allows to identify scattering states. However, this is an expensive strategy which so far has been tested mainly in low-dimensional models and scalar field theories [11,15].

Another interesting challenge is the evaluation of matrix elements for excited states. Here some conceptual problems still have to be addressed, but in principle it should be possible to formulate this problem within the variational approach. A first appetizer of what the lattice could achieve in this direction is the calculation of the decay constant for  $\pi(1300)$  presented in [16].

**Acknowledgements:** I would like to thank D. Brömmel, T. Burch, J. Danzer, L. Glozman, C. Hagen, D. Hierl, M. Limmer, C.B. Lang, D. Mohler, S. Prelovsek, S. Schaefer and A. Schäfer, who I have collaborated with on excited hadron physics over the last few years. Some of the results presented here were obtained on the parallel computers at the Leibniz Rechenzentrum, Garching, and at the ZID, Universität Graz.

## References

1. P.H. Ginsparg, K.G. Wilson, Phys. Rev. D **25** (1982) 2649.
2. S. Sasaki, T. Blum, S. Ohta, Phys. Rev. D **65** (2002) 074503; J.M. Zanotti *et al.*, Phys. Rev. D **65** (2002) 074507; W. Melnitchouk *et al.*, Phys. Rev. D **67** (2003) 114506; J.M. Zanotti *et al.*, Phys. Rev. D **68** (2003) 054506;
3. N. Mathur *et al.*, Phys. Lett. B **605** (2005) 137; S. Sasaki, Prog. Theor. Phys. Suppl. **151** (2003) 143; D. Brömmel *et al.*, Phys. Rev. D **69** (2004) 094513; C.R. Allton *et al.*, Phys. Rev. D **70** (2004) 014501; D. Guadagnoli, M. Papinutto, S. Simula, Phys. Lett. B **604** (2004) 74; B.G. Lasscock *et al.*, Phys. Rev. D **76** (2007) 054510; R. Frigori *et al.*, PoS(LATTICE 2007)114 [arXiv:0709.4582 [hep-lat]].
4. T. Burch *et al.*, Phys. Rev. D **70** (2004) 054502.
5. T. Burch *et al.*, Phys. Rev. D **73** (2006) 017502.
6. T. Burch *et al.*, Phys. Rev. D **73** (2006) 094505.
7. T. Burch *et al.*, Phys. Rev. D **74** (2006) 014504.
8. S. Basak *et al.*, Phys. Rev. D **72** (2005) 074501; Phys. Rev. D **72** (2005) 094506; arXiv:0709.0008 [hep-lat]; D.C. Moore, G.T. Fleming, Phys. Rev. D **74** (2006) 054504.
9. C. Gattringer *et al.*, PoS(LATTICE 2007)123 [arXiv:0709.4456 [hep-lat]].
10. C. Best *et al.*, Phys. Rev. D **56** (1997) 2743; C. Alexandrou *et al.*, Nucl. Phys. B **414** (1994) 815; C.R. Allton *et al.*, Phys. Rev. D **47** (1993) 5128.
11. C. Michael, Nucl. Phys. B **259** (1985) 58.
12. M. Lüscher, U. Wolff, Nucl. Phys. B **339** (1990) 222.
13. M. Asakawa, T. Hatsuda, Y. Nakahara, Prog. Part. Nucl. Phys. **46** (2001) 459; G.P. Lepage, Nucl. Phys. (Proc. Suppl.) **106** (2002) 12; G. Fleming PoS(LATTICE 2007)096; G.M. von Hippel, R. Lewis, R.G. Petry, PoS(LATTICE 2007)043 [arXiv:0710.0014 [hep-lat]]; H.W. Lin, S.D. Cohen, arXiv:0709.1902 [hep-lat].
14. C. McNeile, PoS(LATTICE 2007)019 [arXiv:0710.0985 [hep-lat]].
15. M. Lüscher, Nucl. Phys. B **364** (1991) 237; Nucl. Phys. B **354** (1991) 531.
16. C. Gattringer, C.B. Lang, Nucl. Phys. B **391**, 463 (1993); Phys. Lett. B **274**, 95 (1992); M. Göckeler *et al.*, Nucl. Phys. B **425** (1994) 413; K. Rummukainen, S.A. Gottlieb, Nucl. Phys. B **450** (1995) 397; S. Aoki *et al.*, Phys. Rev. D **67** (2003) 014502; J. Danzer, C. Gattringer, PoS(LATTICE 2007)092, [arXiv:0710.1711 [hep-lat]].
17. C. McNeile, C. Michael, Phys. Lett. B **642** (2006) 244.